Inflammation
https://doi.org/10.1007/s10753-023-01784-8

ORIGINAL ARTICLE

Inhibition of SHP2 by the Small Molecule Drug SHP099 Prevents Lipopolysaccharide-Induced Acute Lung Injury in Mice

Shuhui Ye[1,2] , Bowen Zuo[1,3] , Lenan Xu[1,2] , Yue Wu[1,2] , Ruixiang Luo[1,2] , Lin Ma[1,2] , Wanxin Yao[1,3] , Lingfeng Chen[1,2] , Guang Liang[1,2,4] and Yanmei Zhang[1,3,4]

Received 6 September 2022; accepted 12 January 2023

Abstract— Excessive pulmonary inflammation in acute lung injury (ALI) causes high patient mortality. Anti-inflammatory therapy, combined with infection resistance, can help to prevent ALI and save lives. The expression of Src homology-2 domain-containing protein tyrosine phosphatase 2 (SHP2) was found to be significantly higher in macrophages and lung tissues with ALI, and SHP2-associated MAPK pathways were activated by lipopolysaccharide (LPS). The knockdown of the *SHP2* gene suppressed the LPS-induced release of inflammatory factors and the phosphorylation of regulators in the NF-κB pathways in macrophages. Our findings showed crosstalk between the LPS-induced inflammatory pathway and the SHP2-associated MAPK pathways. SHP2 inhibition could be a valuable therapeutic approach for inhibiting excessive inflammation in ALI. We discovered that giving SHP099, a specific allosteric inhibitor of SHP2, to mice with ALI and sepsis relieves ALI and significantly increases animal survival. Our study highlights the important role of SHP2 in ALI development and demonstrates the potential application of SHP099 for treating ALI.

KEY WORDS: SHP099; SHP2; acute lung injury; erk phosphorylation.

INTRODUCTION

Sepsis and burn infections frequently result in acute lung injury (ALI) and acute respiratory distress syndrome (ARDS). LPS, a known endotoxin found on the outer membrane of gram-negative bacteria, causes neutrophil accumulation, inflammatory cell infiltration, and subsequent inflammatory response. LPS binds to Toll-like receptor 4 (TLR4), triggers downstream cascades, and activates NF-κB signaling to induce inflammation. However, excessive pulmonary inflammation during ALI results in excessive secretion of cytokines such as

The two authors Shuhui Ye and Bowen Zuo contributed equally.

[1]Affiliated Yongkang First People's Hospital and School of Pharmacy, Hangzhou Medical College, Hangzhou 310013, Zhejiang, China
[2]School of Pharmacy, Hangzhou Medical College, Hangzhou 310013, Zhejiang, China
[3]School of Laboratory Medicine and Bioengineering, Hangzhou Medical College, Hangzhou 310013, Zhejiang, China
[4]To whom correspondence should be addressed at and Affiliated Yongkang First People's Hospital and School of Pharmacy, Hangzhou Medical College, Hangzhou, 310013, Zhejiang, China. Email: wzmcliangguang@163.com yanmeizhang@hmc.edu.cn

© The Author(s), under exclusive licence to Springer Science+Business Media, LLC, part of Springer Nature, 2023

Published online: 03 February 2023

TNF-α and IL-6, leukocyte recruitment, high expression of adhesion molecule type 1 (ICAM-1) and vascular cell adhesion molecule-1 (VCAM-1), increased vascular permeability, and diffuse alveolar injury. Anti-inflammatory therapy, combined with infection resistance, can help to prevent ALI and save lives. Because ALI has a high mortality rate, developing therapeutic interventions to prevent excessive inflammation in ALI patients is critical.

Src homology-2 domain-containing protein tyrosine phosphatase (PTP) 2 [SHP2] promotes cell survival and tumorigenesis as well as plays a role in pulmonary inflammation, fibrosis, and diabetes [1–4]. SHP2 regulates allergic and chronic inflammation by activating the PI3K/AKT and ERK signaling pathways [1, 5, 6]. Conversely, SHP2 deficiency alleviates chronic pulmonary inflammation by downregulating myeloid cells [3, 7, 8] and triggers spontaneous pulmonary fibrosis by promoting apoptosis of epithelial cells [9]. SHP2 protects the pulmonary endothelium against barrier permeability [10]. Inhibition or knockdown of SHP2 retained airway epithelial barrier function by suppressing the ERK1/2 MAPK signaling pathway [11]. Integrin beta4-induced antagonistic effect on the SHP2 pathway reduced lung endothelial inflammatory responses [12]. Through the activation of p65-nuclear factor-κB signaling (NF-κB), SHP2 promotes inflammation-driven insulin resistance by triggering monocyte infiltration, reshaping tissue macrophage populations, and regulating the expression of macrophage polarization genes [8, 13]. Although the literature suggests that SHP2 may be a potential therapeutic target for chronic inflammatory diseases, it remains to be seen whether SHP2 inhibition reduces the excessive inflammation seen in ALI.

To avoid the inhibition of other phosphatases, SHP099, an allosteric PTP inhibitor specific to SHP2, was discovered. SHP099 suppresses the RAS-ERK signaling pathway to inhibit receptor tyrosine kinase (RTK)–driven cancer cell proliferation and is efficacious in patient-derived tumor xenograft models [14]. SHP099 suppresses the proliferation of non-small cell lung cancer (NSCLC) cells by inhibiting the ERK signaling pathway. It also inhibits cancer cells showing resistance to anaplastic lymphoma kinase (ALK) inhibitors because of ALK gene rearrangement [15, 16]. Considering the role of SHP2 in activating inflammation and causing pulmonary diseases, it is important to investigate the effect of SHP099 on pulmonary inflammation and ALI.

In the present study, we found that the expression of SHP2 was increased in the lung tissue of mice with ALI. In the LPS-induced ALI mouse model, SHP099 inhibited the inflammatory response. SHP099 inhibited NF-κB phosphorylation and alleviated cytokine expression and release in macrophage cells, resulting in pathological remission in the ALI mouse model. The knockdown of the *SHP2* gene in macrophage cells inhibited the phosphorylation of ERK and suppressed the expression of inflammatory cytokines, thus, validating the effect of SHP099. Thus, our study showed the inhibition effect of SHP099 on excessive pulmonary inflammation and demonstrated the use of SHP099 for treating ALI.

MATERIALS AND METHODS

Animals

Male C57BL/6 mice weighing 18–22 g were obtained from the Animal Centre of Hangzhou Medical College (Hangzhou, China). The mice were housed at constant room temperature with a 12-h light/dark cycle, fed with a standard rodent diet and water, and acclimatized to the laboratory for at least 7 days before their use for studies. The Animal Policy and Welfare Committee at Hangzhou Medical College approved all animal care and experimental procedures.

Construction of an ALI Mouse Model

Twenty-one mice were randomly divided into three groups (control group, LPS treatment group, and SHP099 treatment group). Mice in the SHP099 treatment group received 15 mg/kg SHP099 intraperitoneally for 12 h and 30 min before LPS injection. For treatments, all groups received the same volume of solution. After isoflurane anesthesia, LPS (5 mg/kg) was injected into the trachea to induce ALI. The negative control group was injected with the same amount of saline. After 6 h, chloral hydrate anesthesia was performed on the animals, and the eyeballs were removed to collect serum. The spine was dislocated, and the lungs were washed with PBS to obtain bronchoalveolar lavage fluid (BALF). The remaining lungs were subsequently used for morphological investigation and molecular biology experiments.

Construction of a Sepsis Mouse Model

Eighteen mice were randomly divided into three groups (control group, LPS group, and SHP099 group).

The SHP099 group was intraperitoneally injected with 15 mg/kg SHP099 solution at 12 h and 30 min before LPS treatment. The same amounts of solutions were injected into the negative control group and the LPS positive group. The LPS and SHP099 groups were treated with 32 mg/kg LPS through tail vein injection [17–19]. The same volume of saline was given to the control group. The survival rate was calculated after 11 days of continuous observation of the treated mice.

Cell Culture and Transfection

RAW 264.7 cells were purchased from ATCC. The cells were cultured in DMEM (Cat. #D6429, Sigma-Aldrich, MO, USA) supplemented with 10% fetal bovine serum (FBS, Cat. #FSP500, ExCell Bio) at 37 °C in a 5% CO_2 incubator. The cells were then seeded onto 6-well plates containing an antibiotic-free medium the day before transfection, and knockdown of *SHP2* was performed using Lipofectamine RNAiMAX (Cat. #13778150, Thermo Fisher Scientific, MA, USA). The siRNAs were synthesized by GenePharma (GenePharma, Shanghai, China) and are listed in Table 1.

RNA Extraction and Quantitative Real-Time PCR Assay

TRIzol (Cat. #T9424, Sigma-Aldrich, St. Louis, MO, USA) was used to extract RNA, and the concentration was determined using a NanoDrop 2000 spectrophotometer (Thermo Scientific, USA). One microgram of RNA was reverse transcribed to cDNA according to the manufacturer's protocol (Cat. #11141ES60, YEASEN, Shanghai, China). The expression levels of genes were measured by the relative quantification method using SYBR Green Master Mix (Cat. #11201ES08, YEASEN). Quantitative PCR (qPCR) amplifications were performed on the CFX Connect real-time system (Bio-Rad, Hercules, CA). The primers used in this study are listed in Table 1.

Histopathology and Immunofluorescence Assays

Lung tissues were fixed with 4% paraformaldehyde and then paraffin-embedded, sectioned, and subjected to hematoxylin and eosin (H&E) staining by Haoke Biologicals (www.haokebio.com, Hangzhou, China). Frozen slices of lung tissues and Cell Culture Slides were prepared, fixed with 4% paraformaldehyde, permeabilized with Triton X-100 (Cat. #P1080, Solarbio Science & Technology Co. Ltd., Beijing, China), blocked with 1% BSA for 1 h at room temperature, incubated with primary antibodies overnight at 4 °C, washed with PBS for three times, and incubated with fluorescent secondary antibodies for 30 min and with DAPI (0.5 μg/mL) for 10 min. Photographs were captured using an inverted fluorescence microscope (EVOS M7000, Invitrogen, Carlsbad, CA, USA). Cell Signaling Technology supplied antibodies against SHP2 (Cat. #3397S) and P65 (Cat. #8242 T) (Danvers, MA, USA). ImageJ was used to process fluorescence images (NIH, Bethesda, MD, USA).

Table 1 The Nucleotides Used in This Study

Primer/siRNA	Forward (5′ to 3′)	Reverse (5′ to 3′)	Application
IL-6	GAGGATACCACTCCCAACAGACC	AAGTGCATCATCGTTGTTCATACA	qPCR
IL-1β	CCACAGACCTTCCAGGAGAATG	GTGCAGTTCAGTGATCGTACAGG	qPCR
TNF-α	TGATCCGCGACGTGGAA	ACCGCCTGGAGTTCTGGAA	qPCR
ICAM	AAACCAGACCCTGGAACTGCAC	GCCTGGCATTTCAGAGTCTGCT	qPCR
VCAM	GCTATGAGGATGGAAGACTCTGG	ACTTGTGCAGCCACCTGAGATC	qPCR
β-ACTIN	CCGTGAAAAGATGACCCAGA	TACGACCAGAGGCATACAG	qPCR
SHP2 siRNA	GCAGCUGAAAGAGAAGAAUTT	AUUCUUCUCUUUCAGCUGCTT	Knockdown
Negative siRNA	UUCUCCGAACGUGUCACGUTT	ACGUGACACGUUCGGAGAATT	Knockdown

Myeloperoxidase Activity Assay

The myeloperoxidase (MPO) detection kit (Cat. #A044, Nanjing Jiancheng Bioengineering Institute, Nanjing, China) was used to measure the activity of MPO in the lung tissues of each group.

Enzyme-Linked Immunosorbent Assay (ELISA)

The collected serum, bronchoalveolar lavage fluid (BALF), and tissue proteins of each mice group were analyzed to detect TNF-α and IL-6 by ELISA. The ELISA kits were purchased from Invitrogen (Cat. #88–7064 and #88-7324, Invitrogen).

Isolation of Mouse Primary Peritoneal Macrophages

A 6% broth solution was prepared by sterilization in an autoclave. Next, 2–3 mL of the broth solution was injected intraperitoneally in male C57BL/6 mice. The mice were sacrificed by cervical dislocation after 48–72 h of normal feeding, and the peritoneal cavity was washed repeatedly with serum-free RPMI-1640 medium (Cat. #R8758, Sigma-Aldrich) to collect peritoneal macrophages. After cell counting, the cells were resuspended in RPMI-1640 complete medium (containing 10% FBS, 50 U/mL penicillin, and 50 mg/mL streptomycin) and plated onto cell culture dishes. After 2 h of the cells were placed in a 37 °C cell incubator with 5% CO_2, the mouse primary peritoneal macrophages (MPMs) were completely adherent, and the medium was then replaced with RPMI-1640 complete medium for overnight culture.

Protein extraction and Preparation

A total of 10^6 cells were cultured in a 6-well plate. The pre-cooled protein extraction reagents (containing PMSF and phosphatase inhibitors) were added to the wells. The cells were lysed on ice for 10 min and then further with 30% power by 10 times of ultrasound with the frequency of 1 s on and 2 s off. The lysed cells were centrifuged at 15,000 g for 15 min at 4 °C. The absorbance value was measured in a microplate reader using Coomassie brilliant blue (Cat. #5000205, Bio-Rad) at 595 nm, and the protein concentration was calculated using the standard curve. A 5 × SDS protein loading buffer was used for preparing protein samples, and 40 μg protein in 20 μL volume of each sample was heated at 100 °C water bath for 10 min for denaturation. The protein samples were used for western blotting assays.

Western Blotting Assay

Tissue protein extraction: The lung tissue was placed in a 1.5 mL EP tube. Steel beads and pre-cooled protein extraction reagents (containing PMSF and a phosphatase inhibitor) were added, and the mixture was homogenized at 60 Hz for 120 s with a Scientz-48 homogenizer (Scientz, Ningbo, China). After homogenization, the steel beads were removed, and the samples were centrifuged at 15,000 g for 15 min at 4 °C. Protein concentrations in the samples were measured using a Coomassie brilliant blue kit (Cat. #5000205, Bio-Rad) with a microplate reader at the wavelength of 595 nm. The protein concentration was determined using the standard curve. Denatured and analyzed samples containing 70 μg protein in a volume of 20 μL.

The prepared protein samples were separated by SDS-PAGE and transferred on a 0.45 μm PVDF membrane. After blocking the PVDF membrane with 5% milk or 5% BSA for 1 h, the membrane was incubated overnight with primary antibodies at 4 °C, washed with PBS, incubated further with secondary antibodies, washed again with PBS, and then subjected to development with ECL reagent (Cat. #P10300, NCM Biotech, Jiangsu, China). Antibodies against ERK (Cat. #4695S), p-ERK (Cat. #4695S), p-p65 (Cat. #3033), p65 (Cat. #8242), p-IκB-α (Cat. #2859), IκB-α (Cat. #4812S), and SHP2 (Cat. #3397S) were purchased from Cell Signaling Technology (Danvers, MA, USA). ImageJ software was used to process and quantify the band density (NIH, Bethesda, MD, USA).

Statistical Analysis

Data from three or more independent experiments were expressed as mean ± standard error (mean ± SEM). ANOVA and normality tests were routinely performed, and a *t*-test was used to analyze the difference in the mean value of the two groups. Each *in vitro* experiment included at least three replicates. GraphPad Prism 8.0 was used for graphical analysis, and $P < 0.05$ indicated a statistically significant difference.

RESULTS

SHP2 Expression was Induced in Lung Tissues of Mice with ALI

Figure 1A depicts the establishment of the ALI mouse model. ALI resulted in pulmonary inflammatory cell infiltration and thickening of the alveolar wall. To validate the ALI model, the expression and secretion levels of ICAM, VCAM, and several inflammatory factors were measured. ICAM and VCAM mRNA expression levels were increased (Fig. 1B). The ELISA assays revealed an increase in TNF-α and IL-6 expression in both BALF and serum samples (Fig. 1C). Many erythrocytes accumulated in the pulmonary capillaries and pulmonary septum, along with fibrin exudation in the local alveolar cavity, and the normal alveolar structure was lost (Fig. 1D). Elevated expression of *SHP2* was detected in ALI tissues in the immunofluorescence assay, together with the emergence of CD68-positive macrophages (Fig. 1E). *SHP2* mRNA expression was upregulated in ALI tissues (Fig. 1F).

SHP099 Inhibited LPS-Induced Activation of the SHP2 Signaling Pathway

MPM cells subjected to LPS treatments for 15 min to 1 h showed SHP2 upregulation and ERK phosphorylation.

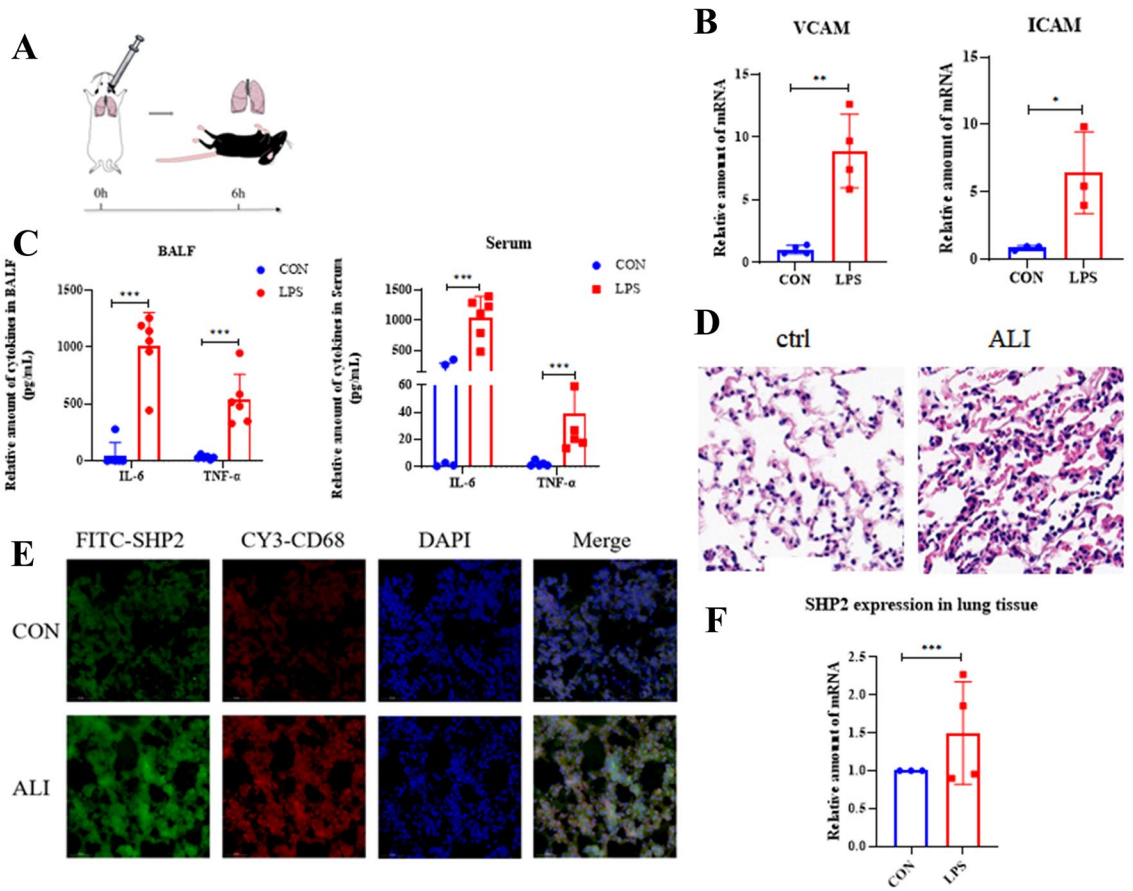

Fig. 1 SHP2 was induced in ALI. **A** Establishment of the mouse ALI model by tracheal instillation of LPS (5 mg/kg). After 6 h of LPS treatment, the mice were anesthetized and sacrificed by spinal dislocation. BALF and lung tissue samples were collected. **B** The right lower lobe of the mice lungs was homogenized for RNA extraction, and qPCR was performed to detect the expression levels of ICAM and VCAM. **C** BALF and serum samples collected from mice were subjected to ELISA to detect the secretion of the cytokines IL-6 and TNF-α. **D** The middle lobes from the right lungs of mice were fixed with paraformaldehyde for histological examination. **E** SHP2 expression in lung macrophages detected by immunofluorescence of CY3 as a marker for CD68 was used to detect macrophages. FITC-labeled SHP2 was used to detect the expression and localization of SHP2. **F** *SHP2* expression in ALI lung tissues was detected by qPCR. Data are expressed as mean ± SEM. * $p < 0.05$, ** $p < 0.01$, *** $p < 0.001$.

This finding suggested that LPS treatment induced the activation of the SHP2 pathway (Fig. 2A). To confirm the activation of SHP2 by LPS, *SHP2* knockdown was performed in RAW 264.7 cells by using siRNA (Fig. 2B). SHP099 treatment was then performed to inhibit SHP2 signaling. The results confirmed that SHP099 inhibited the phosphorylation of AKT and ERK induced by LPS treatment (Fig. 2C).

SHP099 Treatment Suppressed Inflammation

To determine whether SHP099 treatment could suppress LPS-induced inflammation, the expression of cytokines in RAW 264.7 cells with *SHP2* knockdown was examined. The results revealed that LPS-induced inflammation was blocked by SHP099 treatment (Fig. 3A).

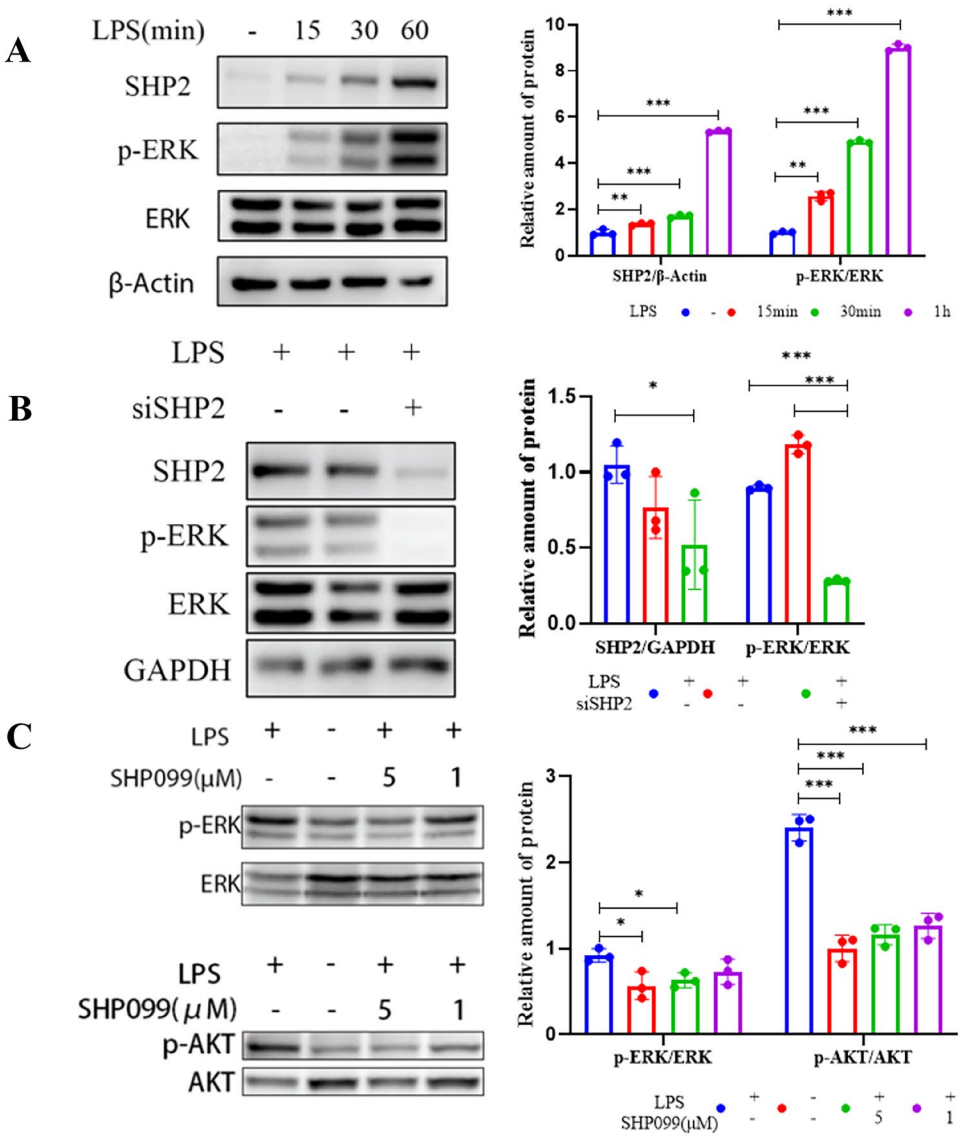

Fig. 2 SHP099 inhibited LPS-induced activation of the SHP2 signaling pathway. **A** LPS was used to treat MPM cells for different periods from 15 min to 1 h. SHP2 expression and ERK phosphorylation were assessed by western blotting assay. **B** *SHP2* knockdown was performed in RAW 264.7 cells by siRNA targeting *SHP2*. LPS treatment was then performed to induce inflammation. ERK phosphorylation was then assessed. The knockdown efficiency was validated. **C** SHP099 at 1 or 5 μM was used to inhibit LPS-induced phosphorylation of ERK and AKT. Values are mean ± SEM, ($n = 3$ per group). * $p < 0.05$, ** $p < 0.01$, *** $p < 0.001$.

SHP099 treatment inhibited inflammation in MPM cells, according to a validation experiment (Fig. 3B). SHP099 treatment reduced the phosphorylation of the p65 protein induced by LPS stimulation in RAW 264.7 cells (Fig. 3C). Furthermore, the immunofluorescent localization of NF-κB showed that SHP099 reduced LPS-induced nuclear translocation of the p65 subunit (Fig. 6D). These results confirmed that SHP099 has an effective anti-inflammatory effect at the cellular level.

SHP099 Protected Against LPS-Induced ALI

SHP099 was administered to the ALI mice model to validate its effect *in vivo* based on evidence that it inhibited LPS-induced activation of the SHP2 and NF-κB pathways and suppressed subsequent cytokine expression and secretion (Fig. 4A). Following LPS treatment, the pulmonary air-blood barrier was damaged, alveolar-capillary permeability increased, and a large number of inflammatory cells infiltrated into the lung interstitium and alveoli, as observed in the successful ALI model. However, SHP099 treatment reversed the pulmonary structure damage (Fig. 4B). BALF was collected as an indicator to measure the degree of lung injury. The total cell number and protein concentration in BALF showed that SHP099 alleviated pulmonary damage (Fig. 4C, D). The expression levels of cytokines IL-6 and TNF-α in BALF and serum were measured by ELISA. Compared to LPS-induced intense inflammatory reaction, SHP099 treatment inhibited the release of cytokines to approximately half of the extent achieved on LPS treatment (Fig. 4E, F).

SHP099 Attenuates Inflammation in ALI Tissues

The levels of IL-6 and TNF-α in the lung tissue homogenate were detected by ELISA. Compared to the nontreated negative control group, the ALI model group showed a significant increase in IL-6 and TNF-α levels, but SHP099 suppressed the release and expression of these cytokines (Fig. 5A). The same results were found

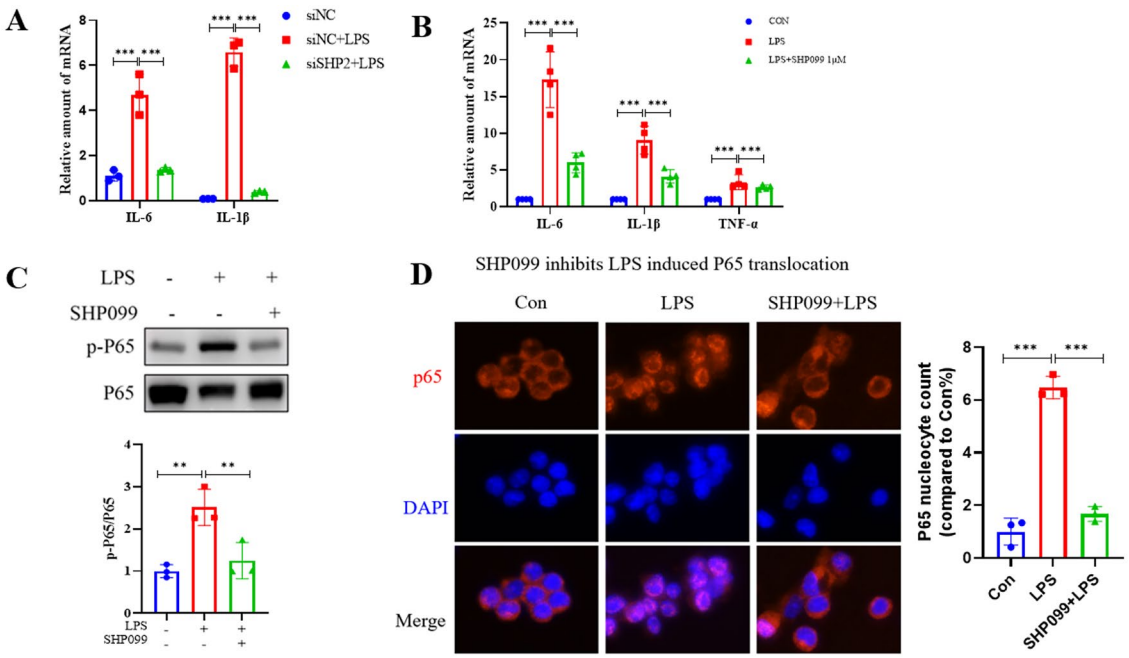

Fig. 3 **A** RAW 264.7 cells were transfected with the negative control siRNA (siNC) or SHP2 siRNA (siSHP2), and the mRNA levels of inflammatory cytokines after LPS (1 μg/mL) stimulation were detected by qPCR. **B** MPM cells were subjected to extraction, and the mRNA expression levels of inflammatory cytokines after LPS (1 μg/mL) stimulation were detected by qPCR. RAW 264.7 cells were pretreated with SHP099 (1 μM) for 1 h and then incubated with LPS for 1 h. **C** Protein levels of phosphorylated p65 were measured by western blotting assay. **D** Representative images of immunofluorescence staining of p65. SHP099 (5 μM) also inhibited the nuclear translocation of the p65 subunit in LPS-induced RAW 264.7 cells. Data are expressed as mean ± SEM, ($n = 3$ per group). * $p < 0.05$, ** $p < 0.01$, *** $p < 0.001$.

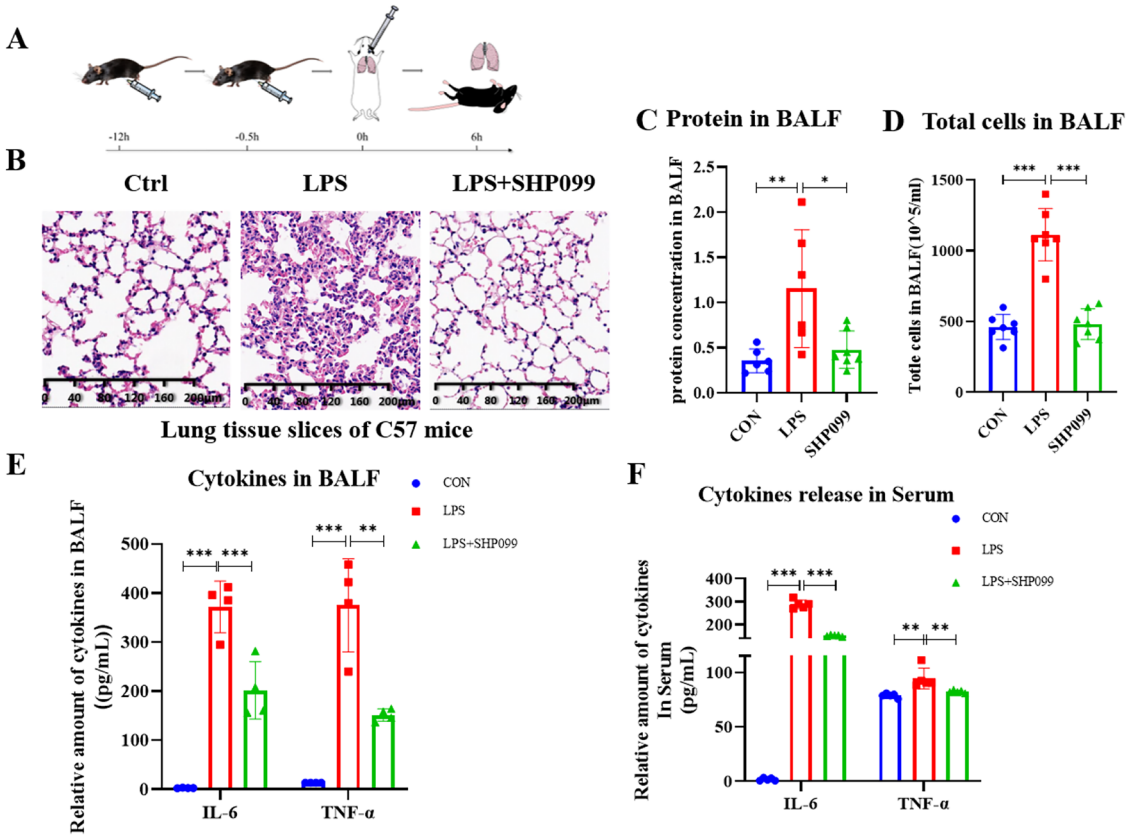

Fig. 4 SHP099 protects against LPS-induced ALI. **A** Mouse disease model and medication schedule. SHP099 (15 mg/kg) was injected intraperitoneally at 12 h and 30 min before the establishment of the model. After 6 h of establishing the model, the mice were sacrificed under anesthesia. BALF, serum, and lung tissue samples were collected from each mouse group. **B** Lung tissue from the right middle lobe of mice was fixed with paraformaldehyde and subjected to HE staining. The BALF sample was collected and centrifuged, and protein concentration in the supernatant was detected (**C**). The cells in the pellet were resuspended and counted (**D**). The expression levels of the inflammatory cytokines TNF-α and IL-6 in BALF supernatant (**E**) and serum (**F**) were detected by ELISA. Data are expressed as mean ± SEM, ($n = 6$ per group). * $p < 0.05$, ** $p < 0.01$, *** $p < 0.001$.

at the mRNA level in the lung tissue (Fig. 5B). This evidence demonstrates that SHP099 protects against LPS-induced inflammation in ALI lung tissues. Neutrophil accumulation is essential for host defense and is a pathological feature of bacterial infections. Excessive neutrophil accumulation leads to lung damage [20]. MPO activity is specific for validating neutrophil infiltration and is usually used as a marker for detecting inflammatory damage. In the present study, the MPO activity increased remarkably in the LPS-treated group but declined significantly in the SHP099-treated group (Fig. 5C). The phosphorylation of ERK, IκB, and NF-κB in ALI lung tissues was then examined. LPS promoted ERK phosphorylation as well as IκB and NF-κB phosphorylation. SHP099 treatment, on the other hand, inhibited this phosphorylation which was consistent with the findings in cultivated cells (Fig. 2). The current study found that SHP099 reduced inflammation in ALI tissues (Fig. 5D).

SHP099 Suppresses LPS-Induced Sepsis

As ALI is a severe illness that causes approximately 30–45% of deaths in patients [21], the influence of SHP099 on the lifespan of mice with acute inflammation was determined. An intravenous injection of 32 mg/kg LPS was used to create a sepsis mouse model. Following that, daily intraperitoneal injections of 15 mg/kg SHP099 were administered. The mortality rate of the SHP099-treated group was significantly lower than that of the sepsis model group during the 11-day monitoring period

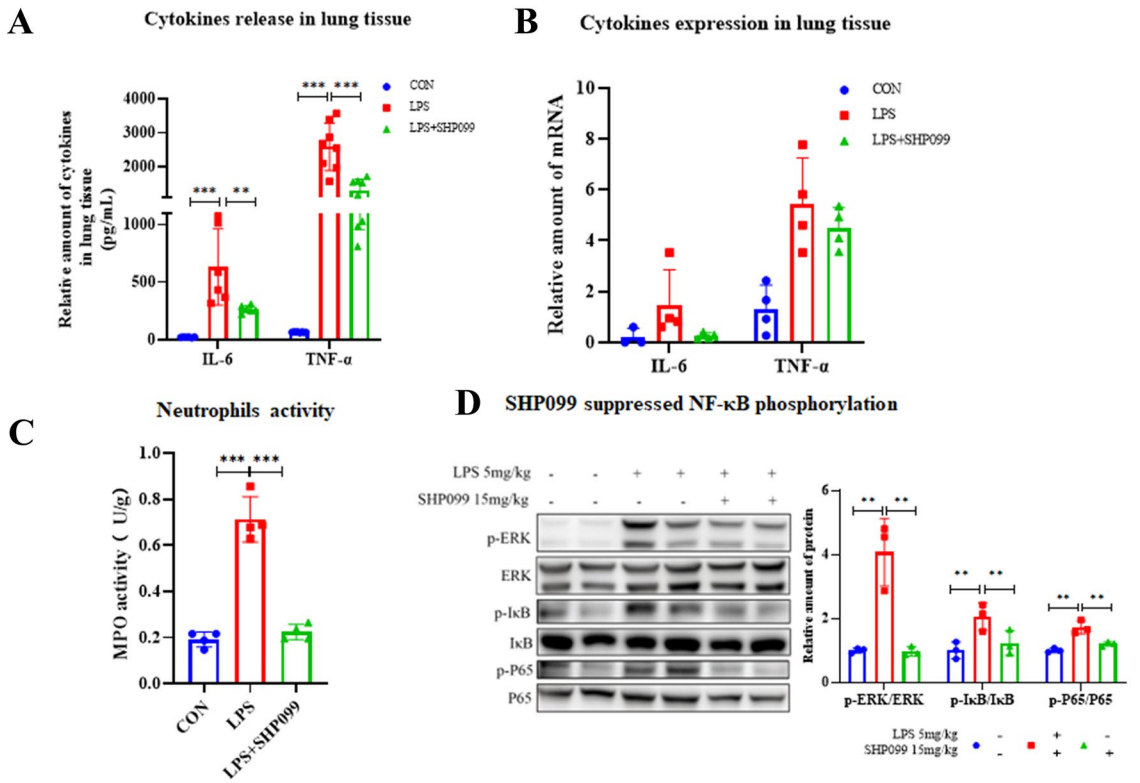

Fig. 5 SHP099 attenuates inflammation in ALI. **A** The expression levels of the inflammatory cytokines TNF-α and IL-6 in lung tissue samples were detected by ELISA ($n=7$ per group). **B** IL-6 and TNF-α expression levels in ALI lung tissues were determined by qPCR. **C** SHP099 inhibited the LPS-induced MPO activity in lung tissues. **D** SHP099 inhibited the NF-κB pathway. NF-κB activation was determined by measuring p-IκB and p-p65 levels. Data are expressed as mean ± SEM. * $p<0.05$, ** $p<0.01$, *** $p<0.001$.

(Fig. 6A). SHP099 significantly improves the survival of mice with acute bacterial inflammation, according to our findings. This is consistent with the finding that SHP099 resists severe inflammatory response induced by LPS in ALI (Fig. 5). These findings demonstrate the protective effect of SHP099 on LPS-induced ALI.

DISCUSSION

LPS is a component of the cytoderm of gram-negative bacteria [22, 23]. It stimulates the tyrosine kinase TLR4 to activate the classic intracellular pathway of NF-κB [22, 24–27]. SHP2 is a member of the classical nonreceptor PTP family, encoded by the *PTPN11* gene [28], and plays many roles in cancer [29, 30], Noonan syndrome [31], skeletal development [31, 32], and hematopoietic cell development [33]. However, the relationship between SHP2 and inflammation has received little attention from researchers. Our present study demonstrated that SHP2 regulates LPS-induced activation of TLR4-associated NF-κB pathways. We also discovered that LPS causes Erk and Akt phosphorylation in SHP2-associated cells (Fig. 2). Therefore, our findings suggest that SHP2 and TLR4 interact and influence one another.

SHP2 catalyzes phosphatase, which is a key intracellular regulator of RTKs on the cell membrane [34]. SHP2 is essential for activating ERK-MAPK signaling [35] and the growth factor-mediated Ras-Raf-ERK pathway in most RTK-related signaling pathways. The phosphatase activity of SHP2 is critical for Ras-Raf-ERK. SHP2 also regulates the PI3K-AKT [36] and JAK/STAT pathways [32]. Our present study demonstrated that LPS induced Akt and Erk phosphorylation by SHP2, which confirmed that LPS can activate SHP2.

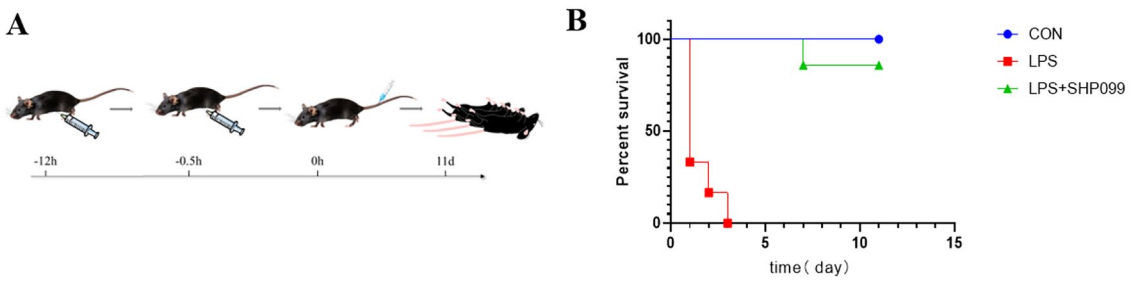

Fig. 6 SHP099 suppresses LPS-induced sepsis. **A** SHP099 increases the survivals of animals with LPS-induced sepsis. The SHP099 treatment group was intraperitoneally injected with 15 mg/kg SHP099 at 12.5 h and 0.5 h before LPS injection. 32 mg/kg LPS was injected through the tail vein to induce sepsis. **B** The survivals of mice were observed every 12 h for 11 days.

SHP099 is Novartis' first allosteric inhibitor of SHP2 and has no significant activity against other PTP families (including SHP1) or kinases with an aminopyrazine compound as their parent core. SHP099 binds simultaneously to the interface of N-terminal SH2, C-terminal SH2, and PTP domains, thus, inhibiting SHP2 activity through an allosteric mechanism [14]. SHP099 suppresses RAS-ERK signaling to inhibit RTK-driven proliferation of human cancer cells *in vitro* and is effective in a mouse tumor xenograft model [14, 37]. Our results confirmed that SHP099 inhibits both LPS-induced inflammation and MAPK activation. Animal experiments reconfirmed the suppressive effect of SHP099 on inflammation.

ALI leads to high mortality [38], which can be considered the early stage of ARDS, which usually leads to sudden respiratory failure and death [39, 40]. Effective diagnosis and treatment of ALI is the key strategy to save patients with ALI [38]. There are currently no specific drugs that target the pathogenesis of acute lung injury, and the main treatment methods are primary lesion treatment and respiratory support therapy, and many researchers are attempting to find drugs to treat ALI [41]. Finding out the pathogenesis of acute lung injury and developing targeted drugs for specific targets is clinically significant [42]. In the present study, we found that the SHP2 level increased in ALI tissues, which is consistent with Dawei Wang's findings in rats and NR8383 Cells [43]. They found suppression of Shp2 can attenuate the M1 polarization, which contributed to suppression of cell inflammation and attenuation of ALI progression, indicating that SHP2 is the potential target for ALI therapy. As macrophage cells are important for inducing inflammation [44], the expression of SHP2 in mice macrophages was investigated in our present study and was found to increase significantly. Therefore, SHP2 in macrophages could be a therapeutic target. Several SHP099-based small molecule allosteric SHP2 inhibitors are currently in clinical trials and have demonstrated promising therapeutic effects in metastatic head and neck cancer, advanced solid tumors, metastatic colorectal cancer, metastatic esophageal cancer, and other cancers. Indeed, we observed that SHP099 treatment significantly prevented ALI and prolonged the survival rate of animals with sepsis.

Actually, there are several limitations to this study. Although the mice sepsis model created by tail vein injection of LPS can demonstrate the effect of the small molecule inhibitor SHP099 on inflammation, other effective animal models of sepsis exist, including intravascular live bacteria, bacterial peritonitis, cecal ligation and perforation, and others [45, 46]. These models can reflect important aspects of sepsis, but the occurrence of sepsis in the human body is a very complex process. If additional research is required, several animal models can be tested at the same time to understand the role and mechanism of SHP099 in the pathogenesis of sepsis.

In summary, the present study demonstrates the critical role of SHP2 in LPS-induced inflammation in macrophages. ALI and sepsis were relieved using the SHP-2-specific inhibitor SHP099. Our findings regarding anti-inflammatory effects of SHP099 in both cells and animals may also provide more useful information for the future use of SHP2 inhibitors in a variety of clinical treatments, as well as the potential application of SHP099 to treat ALI.

SUPPLEMENTARY INFORMATION

The online version contains supplementary material available at https://doi.org/10.1007/s10753-023-01784-8.

AUTHOR CONTRIBUTION

Yanmei Zhang and Lingfeng Chen designed the experiment; Shuhui Ye, Bowen Zuo, Lenan Xu, Yue Wu, Ruixiang Luo, Lin Ma, Wanxin Yao did the experiment; Shuhui Ye and Bowen Zuo analyzed the date; Shuhui Ye wrote the paper; Yanmei Zhang and Guang Liang revised the paper.

FUNDING

The present study is supported by grants from the National Natural Science Foundation of China (No. 31871393), the Zhejiang Provincial Natural Science Foundation of China (NO. HDMY22H318024), Medical and Health Science and Technology Project of Zhejiang Province (NO. 2022RC128), Foundation of Zhejiang Academy of Medical Sciences to Yanmei Zhang.

AVAILABILITY OF DATA AND MATERIALS

The data used to support the findings of this study are available from the corresponding author upon request.

Declarations

Ethics Approval and Consent to Participate All the experimental protocols in this study were approved by the Institutional Animal Care and Use Committee of Hangzhou Medical College. All authors consent to participate this research.

Consent for Publication All authors consent to publish this article.

Competing Interests The authors declare no competing interests.

REFERENCES

1. Chang, C.J., et al. 2022. SHP2: The protein tyrosine phosphatase involved in chronic pulmonary inflammation and fibrosis. *IUBMB Life* 74 (2): 131–142.
2. Zhang, Y., et al. 2016. Manipulating the air-filled zebrafish swim bladder as a neutrophilic inflammation model for acute lung injury. *Cell Death & Disease* 7 (11): e2470.
3. Ouyang, W., et al. 2020. SHP2 deficiency promotes Staphylococcus aureus pneumonia following influenza infection. *Cell Proliferation* 53 (1): e12721.
4. Ahmed, T.A., et al. 2019. SHP2 drives adaptive resistance to ERK signaling inhibition in molecularly defined subsets of ERK-dependent tumors. *Cell Rep* 26 (1): p. 65–78 e5.
5. Deng, R., et al. 2015. Shp2 SUMOylation promotes ERK activation and hepatocellular carcinoma development. *Oncotarget* 6 (11): 9355–9369.
6. McPherson, V.A., et al. 2009. SH2 domain-containing phosphatase-2 protein-tyrosine phosphatase promotes Fc epsilon RI-induced activation of Fyn and Erk pathways leading to TNF alpha release from bone marrow-derived mast cells. *The Journal of Immunology* 183 (8): 4940–4947.
7. Qiu, Z., et al. 2017. Deletion of Shp2 in bronchial epithelial cells impairs IL-25 production *in vitro*, but has minor influence on asthmatic inflammation *in vivo*. *PLoS ONE* 12 (5): e0177334.
8. Zhao, L., et al. 2016. Shp2 deficiency impairs the inflammatory response against Haemophilus influenzae by regulating macrophage polarization. *Journal of Infectious Diseases* 214 (4): 625–633.
9. Zhang, X., et al. 2012. Loss of Shp2 in alveoli epithelia induces deregulated surfactant homeostasis, resulting in spontaneous pulmonary fibrosis. *The FASEB Journal* 26 (6): 2338–2350.
10. Chichger, H., et al. 2015. SH2 domain-containing protein tyrosine phosphatase 2 and focal adhesion kinase protein interactions regulate pulmonary endothelium barrier function. *American Journal of Respiratory Cell and Molecular Biology* 52 (6): 695–707.
11. Zhang, Y., et al. 2021. Shp2 regulates PM2.5-induced airway epithelial barrier dysfunction by modulating ERK1/2 signaling pathway. *Toxicology Letters* 350: 62–70.
12. Chen, W., J.G. Garcia, and J.R. Jacobson. 2010. Integrin beta4 attenuates SHP-2 and MAPK signaling and reduces human lung endothelial inflammatory responses. *Journal of Cellular Biochemistry* 110 (3): 718–724.
13. Paccoud, R., et al. 2021. SHP2 drives inflammation-triggered insulin resistance by reshaping tissue macrophage populations. *Science Translational Medicine* 13 (591).
14. Chen, Y.N., et al. 2016. Allosteric inhibition of SHP2 phosphatase inhibits cancers driven by receptor tyrosine kinases. *Nature* 535 (7610): 148–152.
15. Kano, H., et al. 2021. SHP2 inhibition enhances the effects of tyrosine kinase inhibitors in preclinical models of treatment-naive ALK-, ROS1-, or EGFR-altered non-small cell lung cancer. *Molecular Cancer Therapeutics* 20 (9): 1653–1662.
16. Dardaei, L., et al. 2018. SHP2 inhibition restores sensitivity in ALK-rearranged non-small-cell lung cancer resistant to ALK inhibitors. *Nature Medicine* 24 (4): 512–517.
17. Tanaka, K.A., et al. 2015. Cystine improves survival rates in a LPS-induced sepsis mouse model. *Clinical Nutrition* 34 (6): 1159–1165.
18. Hao, H., et al. 2017. Farnesoid X receptor regulation of the NLRP3 Inflammasome underlies cholestasis-associated sepsis. *Cell Metabolism* 25 (4): 856–867 e5.
19. Wang, Y., et al. 2015. MD-2 as the target of a novel small molecule, L6H21, in the attenuation of LPS-induced inflammatory response and sepsis. *British Journal of Pharmacology* 172 (17): 4391–4405.
20. Balamayooran, G., et al. 2010. Mechanisms of neutrophil accumulation in the lungs against bacteria. *American Journal of Respiratory Cell and Molecular Biology* 43 (1): 5–16.
21. Matthay, M.A., et al. 2019. Acute respiratory distress syndrome. *Nature Reviews. Disease Primers* 5 (1): 18.
22. Nie, Y., et al. 2019. Dehydrocostus lactone suppresses LPS-induced acute lung injury and macrophage activation through

NF-kappaB signaling pathway mediated by p38 MAPK and Akt. *Molecules* 24 (8).
23. Ding, Y.H., et al. 2019. Isoalantolactone suppresses LPS-induced inflammation by inhibiting TRAF6 ubiquitination and alleviates acute lung injury. *Acta Pharmacologica Sinica* 40 (1): 64–74.
24. Tang, J., et al. 2021. Effect of gut microbiota on LPS-induced acute lung injury by regulating the TLR4/NF-kB signaling pathway. *International Immunopharmacology* 91: 107272.
25. Yang, L., et al. 2021. Cardamonin inhibits LPS-induced inflammatory responses and prevents acute lung injury by targeting myeloid differentiation factor 2. *Phytomedicine* 93: 153785.
26. Shimazu, R., et al. 1999. MD-2, a molecule that confers lipopolysaccharide responsiveness on Toll-like receptor 4. *Journal of Experimental Medicine* 189 (11): 1777–1782.
27. Domscheit, H., et al. 2020. Molecular dynamics of lipopolysaccharide-induced lung injury in rodents. *Frontiers in Physiology* 11: 36.
28. He, R.J., et al. 2014. Protein tyrosine phosphatases as potential therapeutic targets. *Acta Pharmacologica Sinica* 35 (10): 1227–1246.
29. Zhang, J., F. Zhang, and R. Niu. 2015. Functions of Shp2 in cancer. *Journal of Cellular and Molecular Medicine* 19 (9): 2075–2083.
30. Maroun, C.R., et al. 2000. The tyrosine phosphatase SHP-2 is required for sustained activation of extracellular signal-regulated kinase and epithelial morphogenesis downstream from the met receptor tyrosine kinase. *Molecular and Cellular Biology* 20 (22): 8513–8525.
31. Kamiya, N., H.K. Kim, and P.D. King. 2014. Regulation of bone and skeletal development by the SHP-2 protein tyrosine phosphatase. *Bone* 69: 55–60.
32. Song, Z., et al. 2021. Tyrosine phosphatase SHP2 inhibitors in tumor-targeted therapies. *Acta Pharm Sin B* 11 (1): 13–29.
33. Frearson, J.A., and D.R. Alexander. 1997. The role of phosphotyrosine phosphatases in haematopoietic cell signal transduction. *BioEssays* 19 (5): 417–427.
34. Qu, C.K. 2000. The SHP-2 tyrosine phosphatase: Signaling mechanisms and biological functions. *Cell Research* 10 (4): 279–288.
35. Neel, B.G., H. Gu, and L. Pao. 2003. The 'Shp'ing news: SH2 domain-containing tyrosine phosphatases in cell signaling. *Trends in Biochemical Sciences* 28 (6): 284–293.
36. Gu, H., J.D. Griffin, and B.G. Neel. 1997. Characterization of two SHP-2-associated binding proteins and potential substrates in hematopoietic cells. *Journal of Biological Chemistry* 272 (26): 16421–16430.
37. Zhu, G., et al. 2020. Phase separation of disease-associated SHP2 mutants underlies MAPK hyperactivation. *Cell* 183 (2): 490–502 e18.
38. Butt, Y., A. Kurdowska, and T.C. Allen. 2016. Acute lung injury: A clinical and molecular review. *Archives of Pathology and Laboratory Medicine* 140 (4): 345–350.
39. Hughes, K.T., and M.B. Beasley. 2017. Pulmonary manifestations of acute lung injury: More than just diffuse alveolar damage. *Archives of Pathology and Laboratory Medicine* 141 (7): 916–922.
40. Bitterman, P.B. 1992. Pathogenesis of fibrosis in acute lung injury. *The American Journal of Medicine*.
41. He, Y.Q., et al. 2021. Natural product derived phytochemicals in managing acute lung injury by multiple mechanisms. *Pharmacological Research* 163: 105224.
42. Zoulikha, M., et al. 2022. Pulmonary delivery of siRNA against acute lung injury/acute respiratory distress syndrome. *Acta Pharmaceutica Sinica B* 12 (2): 600–620.
43. Wang, D., and Q. Cao. 2022. Shp2 in alveolar macrophages regulates macrophage I phenotype in acute lung injury. *International Journal of Toxicology* 41 (5): 412–419.
44. Xiao, J., et al. 2020. Combined administration of SHP2 inhibitor SHP099 and the alpha7nAChR agonist PNU282987 protect mice against DSSinduced colitis. *Molecular Medicine Reports* 22 (3): 2235–2244.
45. Poli-de-Figueiredo, L.F., et al. 2008. Experimental models of sepsis and their clinical relevance. *Shock* 30 (Suppl 1): 53–59.
46. Ritter, C., et al. 2003. Oxidative parameters and mortality in sepsis induced by cecal ligation and perforation. *Intensive Care Medicine* 29 (10): 1782–1789.

Publisher's Note Springer Nature remains neutral with regard to jurisdictional claims in published maps and institutional affiliations.

Springer Nature or its licensor (e.g. a society or other partner) holds exclusive rights to this article under a publishing agreement with the author(s) or other rightsholder(s); author self-archiving of the accepted manuscript version of this article is solely governed by the terms of such publishing agreement and applicable law.